

$\text{Bi}_2\text{Ca}_2\text{Co}_{1.7}\text{O}_x$ thermoelectric ceramics textured by laser floating zone method

A. SOTELO¹, E. GUILMEAU², M. A. MADRE¹, S. MARINEL², S. LEMONNIER², J. C. DIEZ¹

¹ICMA (UZ-CSIC), Depto. de Ciencia y Tecnología de Materiales y Fluidos, C/María de Luna 3, E-50018, Zaragoza (Spain)

²CRISMAT Laboratory, UMR 6508 CNRS-ENSICAEN, 6 Bld Maréchal Juin, 14050 Caen cedex (France)

Thermoelectric performance on cobaltite ceramics can be increased raising the electrical conductivity. This can be performed by increasing grain size and aligning them along a preferential direction by the Laser Floating Zone (LFZ) method. In this work, $\text{Bi}_2\text{Ca}_2\text{Co}_{1.7}\text{O}_x$ ceramics have been directionally grown at three different speeds, 15, 30 and 50 mm/h. It has been found a small influence of the growth conditions on the thermoelectric properties. In all the cases, the microstructure shows alternated cobaltite layers with small CoO inclusions. In despite, the thermopower is higher than usual in misfit cobaltites obtained by conventional solid state routes. This preliminary result originates probably from oxygen vacancies.

Keywords: Electrical properties, cobaltites, thermoelectric power.

Cerámicas termoeléctricas $\text{Bi}_2\text{Ca}_2\text{Co}_{1.7}\text{O}_x$ texturadas mediante fusión zonal flotante inducida por láser

Las prestaciones termoeléctricas de las cerámicas basadas en óxidos de cobalto pueden ser aumentadas por la disminución de la resistividad eléctrica. Esto puede realizarse aumentando el tamaño de grano y alineándolo en una dirección preferencial, utilizando el método de zona flotante inducida por láser (LFZ). En este trabajo, se han crecido cerámicas termoeléctricas de composición $\text{Bi}_2\text{Ca}_2\text{Co}_{1.7}\text{O}_x$ a tres velocidades diferentes, 15, 30 y 50 mm/h. Se ha encontrado que las condiciones de crecimiento tienen poca influencia en las propiedades termoeléctricas. En todos los casos, la microestructura está formada por capas alternadas de cobaltitas, con pequeñas inclusiones de CoO. A pesar de ello, el poder termoeléctrico medido es mayor de lo habitual para este tipo de materiales preparados por métodos convencionales en estado sólido. Este resultado preliminar está originado, probablemente, por la formación de vacantes de oxígeno.

Palabras clave: Propiedades eléctricas, cobaltitas, poder termoeléctrico.

1. INTRODUCTION

Thermoelectric materials can be used to transform thermal to electrical energy owing to the well-known Seebeck effect. This physical property allows producing electrical power from a thermal gradient between the cold and the hot side of a thermoelectric system. The performance of such materials is quantified by the figure of merit Z , which is defined as $S^2/\rho\kappa$, where S is the Seebeck coefficient, ρ the electrical resistivity, and κ the thermal conductivity. As all these parameters are linked and tend to vary on inverse ways, it is difficult to improve the Z value. The improvement of the conversion efficiency of the thermoelectric system is then carried out by increasing the temperature difference between the hot and the cold side of the system. This is possible when the thermoelectric system can operate at high temperature for long-term use, usually under air. This application can be achieved using thermoelectric oxide ceramics. This is the main reason of the intense research work performed, after the discovery of large thermoelectricity in Na_xCoO_2 (1), to explore new Co oxides exhibiting high thermoelectric performances. Some layered cobaltites, such as $[\text{Ca}_2\text{CoO}_3][\text{CoO}_2]_{1.62}$ and $[\text{Bi}_{0.87}\text{SrO}_{2.2}][\text{CoO}_2]_{1.82}$ were also found to exhibit good thermoelectric (TE) properties (2-5).

The crystal structure of these layered cobaltites is composed of an alternate stacking of a common conductive CdI_2 -type CoO_2 layer with a two-dimensional triangular lattice and a block layer, composed of insulating rock-salt-type (RS) layers (6-8). The two RS and CoO_2 layers have common a and c axes, while the b -axis lengths of the two layers are different. Due to their high structural anisotropy, the alignment of plate-like grains by mechanical and/or chemical processes is necessary to attain macroscopic properties comparable to those obtained on single crystals. It has been established that the Laser Floating Zone (LFZ) technique is adequate to obtain a good grain orientation in several oxide ceramic systems (9-11). With the LFZ processing, a reduction of the electrical resistivity is expected. In this paper, we report the processing of long textured $\text{Bi}_2\text{Ca}_2\text{Co}_{1.7}\text{O}_x$ ceramics by the LFZ technique using different growth rates. The microstructural and phase compositions analyses of the textured ceramics have been performed by scanning electron microscopy (SEM-EDS) and powder X-ray diffraction (XRD). Their thermoelectric properties were also measured as a function of temperature and correlated with the microstructure.

2. EXPERIMENTAL

Polycrystalline ceramics with initial composition $\text{Bi}_2\text{Ca}_2\text{Co}_{1.7}\text{O}_x$ were prepared using the conventional solid-state synthesis technique from commercial Bi_2O_3 (Panreac, 98 + %), CaCO_3 (Panreac, 98 + %) and Co_2O_3 (Aldrich, 98 + %) powders. They were weighed in the adequate proportions, mixed, milled and thermally treated twice at 750 and 800°C for 12h under air, with an intermediate milling, to assure the total elimination of the CO_2 from the metallic carbonates, which could decompose in the LFZ process, leading to bubble formation inside the melt, disturbing the directional ceramic crystallization. The resulting mixture was then cold isostatically pressed at 200 MPa in order to obtain green ceramic cylinders which were subsequently used as feed in a LFZ device (12) equipped with a continuous power Nd:YAG laser (1.06 μm). The growth processes were performed downwards at three different growth rates (15, 30 and 50 mm/h), with no rotation of the seed. To assure compositional homogeneity of the melt, a feed rotation of 15 rpm has been performed. Finally, after the texturing process, long (more than 20 cm) and geometrically homogeneous textured cylindrical rods were obtained.

In order to identify the present phases in the textured materials, powder X-ray diffraction diagrams of the final products were recorded at room temperature using a Siemens Kristalloflex diffractometer, working with Cu K α radiation, and 2θ between 10 and 60 degrees. SEM was performed on transversal and longitudinal polished surfaces, the micrographs were recorded in a JEOL 6000 microscope provided with an energy dispersive spectroscopy (EDS) device. Electrical resistivity measurements were performed using the standard dc four-probe technique at temperatures between 5 and 400K, with no applied external field, in a Physical Properties Measurement System (PPMS) from Quantum Design. Thermopower measurements were performed at temperatures between 5 and 300K in an experimental setup described elsewhere (13).

3. RESULTS AND DISCUSSION

In order to determine the phases in the samples, powder X-ray diffraction of the final textured bars has been recorded. The XRD plots for each growth speed are displayed in figure 1. It can be clearly seen that all the obtained RXD diagrams show the same pattern. Major peaks correspond to the misfit cobaltite $\text{Bi}_2\text{Ca}_2\text{Co}_{1.7}\text{O}_x$ (14).

Figure 2 shows the polished transversal surface of the textured bars. In figure 2a, using backscattered electrons, it can be easily observed the very homogeneous microstructure with a small radial segregation observed in form of a very narrow outer ring (20-30 μm). This zone shows the presence of very small Bi-free secondary phases (dark contrast). The rest of the section is mainly composed by the $\text{Bi}_2\text{Ca}_2\text{Co}_{1.7}\text{O}_x$ phase (light grey contrast) and CoO dendrites homogeneously dispersed into the thermoelectric matrix, as secondary phase. All the studied samples show the absence of residual porosity at this magnification level, as can be seen in figure 2b, using secondary electrons. The absence of porosity will be reflected in a good grains connectivity, which leads to low resistivity values, when compared with samples prepared by the conventional solid state route. Figure 2c shows a close view of the outer ring, where it can be observed the presence of the Bi-free secondary phases (with an stoichiometry close

to the well known $\text{Ca}_3\text{Co}_5\text{O}_9$ phase), easily identified by their growth habit, perpendicular to the outer surface of the as grown bar.

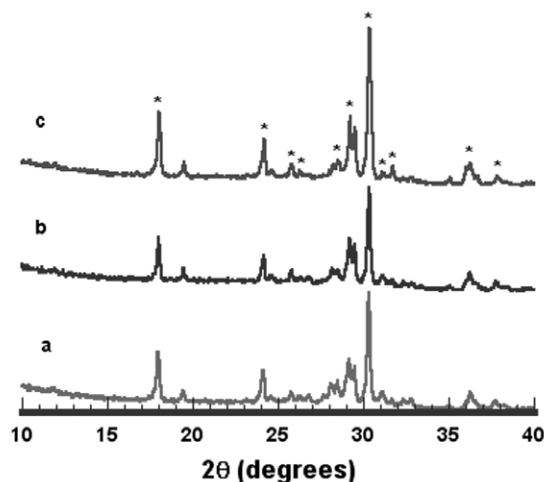


Fig. 1- Powder XRD patterns of the final textured as grown materials at a) 15, b) 30, and c) 50 mm/h. Peaks marked with an * correspond to the misfit cobaltite $\text{Bi}_2\text{Ca}_2\text{Co}_{1.7}\text{O}_x$.

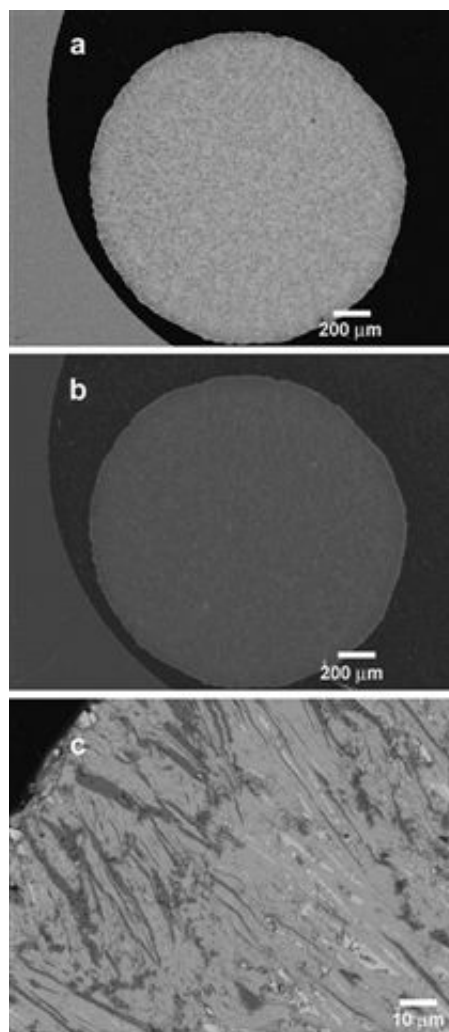


Fig. 2- SEM micrographs of transversal polished sections of a sample growth at 15 mm/h. a) General view, showing the distribution of the secondary phases (dark contrast); b) General view (secondary electrons image), showing the absence of porosity; c) Close view of the external region, showing the outer ring where the Bi-free secondary phases are found (darkest grey contrast).

In figure 3 the polished longitudinal section of the textured bars is displayed. Figure 3a shows the presence of dendritic secondary phases (black contrast), which grow from the outer surface to the inner part of the cylinder. This is indicative of a non-totally plain solidification front. Even in these conditions, a good texture is developed, with the thermoelectric phases well oriented in the growth direction in all the studied samples (see figure 3b). Furthermore, this microstructure pattern has been found independently of the chosen growth speed, which slightly changes the size of the main phases. In figure 3b, three different contrasts are found. The black one has been previously identified as CoO, which shows a very small particle size when compared with the main platelet-like phases (grey contrasts). Furthermore, the cobaltite phase identified by XRD is observed as two different grey contrasts. EDS analyses show that the dark grey grains are Co-rich, while the light ones have a smaller Co content. As it is displayed in figure 3b, these two cobaltite grains appear as alternate layers in the structure.

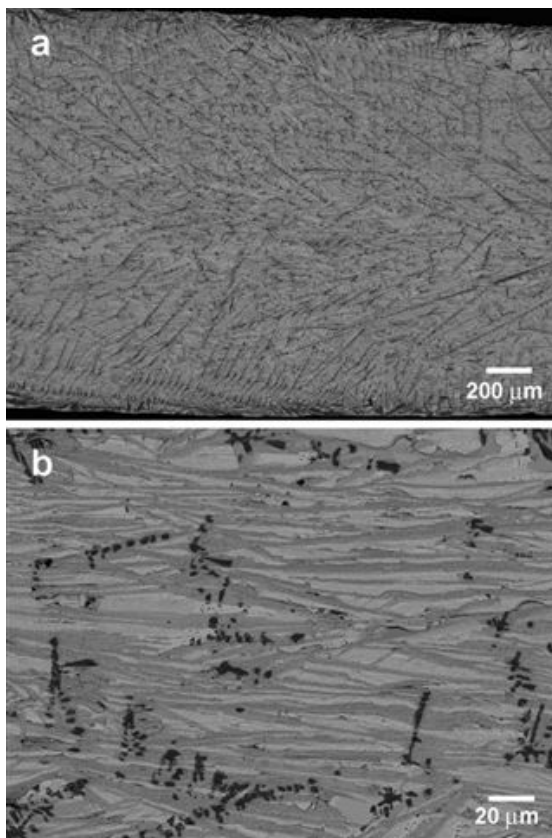


Fig. 3- SEM micrographs of longitudinal polished sections of a sample growth at an intermediate rate of 30 mm/h. a) General view, showing the misorientation and distribution of the CoO secondary phases (black contrast); b) Close view of the bar, showing the multilayer formation by the alternating cobaltite layers (dark and light grey contrasts).

The temperature (T) dependence of the resistivity (ρ) according to the growth rate of the textured materials is shown in figure 4. As it can be easily seen, the $\rho(T)$ curve exhibits a semiconducting behavior from high (400 K) to low temperature (5 K) independently of the growth rate. This semiconducting behavior is in agreement with earlier reports on this cobaltite system (8, 14). The resistivity values decrease when lower growth speeds are used, as a consequence of the better grain alignment and the larger grain sizes. The minimum value at room temperature, for the samples grown

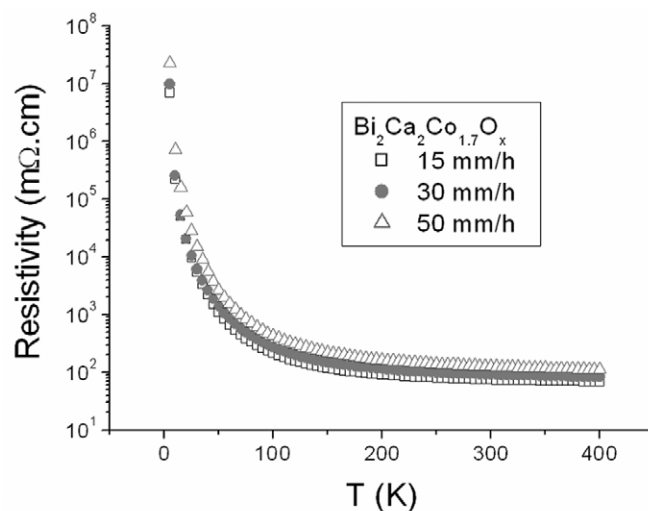


Fig. 4- Temperature dependence of the electrical resistivity, ρ according to the growth rate.

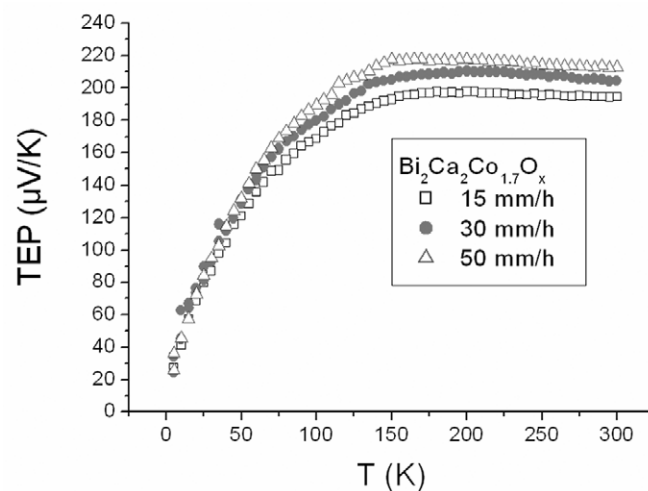


Fig. 5- Temperature dependence of the thermopower according to the growth rate.

at 15 mm/h, is about 60 mΩ.cm, which is lower than the resistivities reported for the sintered specimens (6,8), which show resistivities around 80-100 mΩ.cm.

Figure 5 shows the variation of the thermopower with the temperature, of the as-processed rods. It can be clearly seen that the sign of the thermopower is positive for the entire measured temperature range, which confirms a mechanism involving hole conduction. The values of the thermopower increase with the temperature, with the same behavior for all the samples. It involves an increase from low temperature (5 K) to about 150 K, where a maximum of about 225 $\mu\text{V/K}$ is reached for samples grown at 50 mm/h, which is much higher than those reported for solid state sintered materials (usually around 150 $\mu\text{V/K}$). From 200 K to room temperature, the thermopower value maintains practically constant. The high value of the thermopower (50% higher than those obtained for materials prepared by a conventional solid state reaction) is not common in this system but we can give two explanations to this phenomena: 1) the high thermopower can be associated to the presence of alternate layers with different Co contents as it was previously introduced by microstructure observations, 2) the LFZ growth can probably generate oxygen vacancies in

larger content than in bulk samples synthesized in a classic solid state reaction. The hole concentration is consequently decreased due to the reduction of the cobalt. It has already been evidenced that, at reduced conditions, the misfit phase $[\text{Ca}_2\text{CoO}_3][\text{CoO}_2]_{1.62}$ is not oxygen stoichiometric but contains considerable amounts of oxygen vacancies (15). The decrease of the upper limit value of the thermopower according to the decrease of the growth speed tends to confirm our hypotheses, since the "stoichiometric" cobaltite phase is probably better stabilized and the oxygen vacancies are probably reduced with the decrease of the growth speed. In any cases, we strongly believe that the non stoichiometry is the origin of such an effect and strongly modifies the carrier concentration in the system. Other characterizations have to be performed to confirm these results.

In order to evaluate the thermoelectric performance of these materials, the power factor S^2/ρ has been calculated. The temperature dependence of the power factor (PF), estimated from the data represented in figures 4 and 5 is plotted in figure 6. It can be clearly seen a reduction in the PF when the growth speed increases. The maximum value of, approximately, 0.05 mW/mK² at 300 K for the 15 mm/h sample is reduced to about 0.03 mW/mK² at 300 K, when high growth speed is used (50 mm/h).

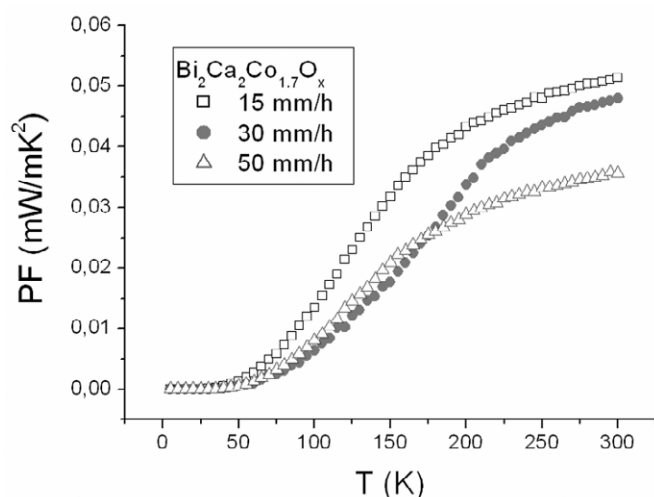


Fig.6- Temperature dependence of the Power factor, S^2/ρ , according to the growth rate.

4. CONCLUSIONS

It has been shown that $\text{Bi}_2\text{Ca}_2\text{Co}_{1.7}\text{O}_x$ thermoelectric materials can be directionally grown by the laser floating zone method for the first time, in our knowledge. This growth process leads to a multilayer cobaltite with small compositional differences between layers, mainly in Co content. In despite of this effect, the measured thermoelectric properties show a decrease on the resistivity values, compared with solid state sintered samples but, more important, a spectacular increase on the thermopower (or Seebeck coefficient) is found. The physical properties measured are in agreement with the literature, resistivity values are decreasing when Seebeck coefficient increases.

ACKNOWLEDGMENTS

The authors wish to thank the Gobierno de Aragón (Consolidated Research Groups T12 and E03) for financial support. The technical contributions of C. Estepa, J.A. Gómez, C. Gallego and R. Lou are also acknowledged.

REFERENCES

1. I. Terasaki, Y. Sasago, K. Uchinokura, Large thermoelectric power in NaCo_2O_4 single crystals, *Phys. Rev. B* 56, 20, 12685-12687 (1997).
2. R. Funahashi, I. Matsubara, H. Ikuta, T. Takeuchi, U. Mizutani, S. Sodeoka, An oxide single crystal with high thermoelectric performance in air, *Jpn. J. Appl. Phys.* 39, 11B, L1127-L1129 (2000).
3. A. C. Masset, C. Michel, A. Maignan, M. Hervieu, O. Toulemonde, F. Studer, B. Raveau, J. Hejtmanek, Misfit-layered cobaltite with an anisotropic giant magnetoresistance $\text{Ca}_2\text{Co}_2\text{O}_7$, *Phys. Rev. B* 62, 1, 166-175 (2000).
4. H. Leligny, D. Grebille, O. Perez, A. C. Masset, M. Hervieu, B. Raveau, A five-dimensional structural investigation of the misfit layer compound $[\text{Bi}_{0.87}\text{SrO}]_2[\text{CoO}_2]_{1.87}$, *Acta Cryst. B* 56, Part 2, 173-182 (2000).
5. A. Maignan, D. Pelloquin, S. Hebert, Y. Klein, M. Hervieu, Thermoelectric Power In Misfit Cobaltites Ceramics: Optimization By Chemical Substitutions, *Bol. Soc. Esp. Ceram. V.* 45, 3, 122-125 (2006).
6. A. Maignan, S. Hébert, M. Hervieu, C. Michel, D. Pelloquin, D. Khomskii, Magnetoresistance and magnetothermopower properties of $\text{Bi}/\text{Ca}/\text{Co}/\text{O}$ and $\text{Bi}(\text{Pb})/\text{Ca}/\text{Co}/\text{O}$ misfit layer cobaltites, *J. Phys.: Condens. Matter.* 15,17, 2711-2723 (2003).
7. H. Itahara, C. Xia, J. Sugiyama, T. Tani, Fabrication of textured thermoelectric layered cobaltites with various rock salt-type layers by using beta- $\text{Co}(\text{OH})_2$ platelets as reactive templates, *J. Mater. Chem.* 14, 1, 61-66 (2004).
8. E. Guilmeau, M. Mikami, R. Funahashi, D. Chateigner, Synthesis and thermoelectric properties of $\text{Bi}_{2.5}\text{Ca}_{2.5}\text{Co}_2\text{O}_x$ layered cobaltites, *J. Mater. Res.* 20, 4, 1002-1008 (2005).
9. Y. Huang, G. F. de la Fuente, A. Sotelo, A. Badía, F. Lera, R. Navarro, C. Rillo, R. Ibáñez, D. Beltran, F. Sapiña, A. Beltran, $(\text{Bi,Pb})_2\text{Sr}_2\text{Ca}_2\text{Cu}_3\text{O}_{10+\delta}$ superconductor composites: Ceramics vs. fibers, *Physica C* 185, Part 4, 2401-2402 (1991).
10. A. Sotelo, E. Guilmeau, M. A. Madre, S. Marinell, J. C. Diez, M. Prevel, Fabrication and properties of textured Bi-based cobaltite thermoelectric rods by zone melting, *J. Eur. Ceram. Soc.* 27, 13-15, 3697-3700 (2007).
11. J. C. Diez, M. A. Madre, A. Sotelo, J. I. Peña, Study of directionally solidified eutectic $\text{Al}_2\text{O}_3\text{-ZrO}_2(3\%\text{Y}_2\text{O}_3)$ doped with TiO_2 , *Bol. Soc. Esp. Ceram. V.* 46, 3, 119-122 (2007).
12. G. F. de la Fuente, J. C. Diez, L. A. Angurel, J. I. Peña, A. Sotelo, R. Navarro, Wavelength dependance in laser floating zone processing. A case study with Bi-Sr-Ca-Cu-O superconductors, *Adv. Mater.* 7, 10, 853 (1995).
13. J. Hejtmanek, Z. Jirak, M. Marysko, C. Martin, A. Maignan, M. Hervieu, B. Raveau, Interplay between transport, magnetic, and ordering phenomena in $\text{Sm}_{1-x}\text{Ca}_x\text{MnO}_3$, *Phys. Rev. B* 60, 20, 14057-14065 (1999).
14. E. Guilmeau, M. Pollet, D. Grebille, D. Chateigner, B. Vertruyen, R. Cloots, R. Funahashi, Neutron diffraction texture analysis and thermoelectric properties of BiCaCoO misfit compounds, *Mater. Res. Bull.* 43, 2, 394-400 (2008).
15. M. Karppinen, H. Fjellvåg, T. Konno, Y. Morita, T. Motohashi, H. Yamauchi, Evidence for oxygen vacancies in misfit-layered calcium cobalt oxide, $[\text{CoCa}_2\text{O}_3](\text{q})\text{CoO}_2$, *Chem. Mater.* 16, 14, 2790-2793 (2004).

Recibido: 31.07.07

Aceptado: 20.12.07